Matter and Radiation at Extremes REVIEW scitation.org/journal/mre

Pressure-induced hydride superconductors above 200 K

Cite as: Matter Radiat. Extremes 6, 068201 (2021); doi: 10.1063/5.0065287
Submitted: 31 July 2021 • Accepted: 15 September 2021 •
Published Online: 6 October 2021

View Online Export Citation CrossMark

Xiaohua Zhang,[1,2] Yaping Zhao,[1] Fei Li,[1] and Guochun Yang[1,2,a)]

AFFILIATIONS

[1]State Key Laboratory of Metastable Materials Science and Technology and Key Laboratory for Microstructural Material Physics of Hebei Province, School of Science, Yanshan University, Qinhuangdao 066004, China
[2]Centre for Advanced Optoelectronic Functional Materials Research and Key Laboratory for UV Light-Emitting Materials and Technology of Ministry of Education, Northeast Normal University, Changchun 130024, China

Note: This paper is a part of the Special Topic Collection on High Pressure Science 2021.
[a)]**Author to whom correspondence should be addressed:** yanggc468@nenu.edu.cn

ABSTRACT

Although it was proposed many years ago that compressed hydrogen should be a high-temperature superconductor, the goal of room-temperature superconductivity has so far remained out of reach. However, the successful synthesis of the theoretically predicted hydrides H_3S and LaH_{10} with high superconducting transition temperatures T_C provides clear guidance for achieving this goal. The existence of these superconducting hydrides also confirms the utility of theoretical predictions in finding high-T_C superconductors. To date, numerous hydrides have been studied theoretically or experimentally, especially binary hydrides. Interestingly, some of them exhibit superconductivity above 200 K. To gain insight into these high-T_C hydrides (>200 K) and facilitate further research, we summarize their crystal structures, bonding features, and electronic properties, as well as their superconducting mechanism. Based on hydrogen structural motifs, covalent H_3S with isolated hydrogen and several clathrate superhydrides (LaH_{10}, YH_9, and CaH_6) are highlighted. Other predicted hydrides with various H-cages and two-dimensional H motifs are also discussed. Finally, we present a systematic discussion of the common features, current problems, and future challenges of these high-T_C hydrides.

I. INTRODUCTION

Room-temperature superconductivity has been one of the most attractive targets in condensed matter physics ever since Kamerlingh Onnes found the superconducting transition of Hg at 4.2 K in 1911.[1] However, the highest superconducting transition temperature T_C that can be achieved by cuprates, the most representative class of unconventional superconductors, is 135 K at ambient pressure,[2] and even at high pressure only reaches as high as 160 K.[3] On the other hand, it has been proposed that under high pressure, solid hydrogen should achieve metallization and high-T_C superconductivity (100–760 K) in either molecular[4–6] or atomic phases,[7,8] based on Bardeen–Cooper–Schrieffer (BCS) theory,[9] although the pressure required is far beyond what can be experimentally achieved.[10,11] Excitingly, however, hydrides are predicted to be able to achieve high-T_C superconductivity at relatively low pressure owing to chemical precompressions,[12] and this has led to an upsurge in research on compressed hydrides.

Thus far, remarkable achievements have been made with pressure-induced superconductivity in hydrides,[13] bringing room-temperature superconductivity within reach. In terms of element category, almost all of the known binary hydrides have been studied theoretically or experimentally.[14–20] On the other hand, a plethora of ternary hydrides exhibiting superconductivity are also being explored, and there is a broad development space in terms of diverse chemical compositions, synergistic charge transfer, and combinations of the merits of different elements.[21–38]

As proposed by Ashcroft,[12] hydrides can achieve superconductivity under much lower pressures than metallic hydrogen. Following this principle, numerous hydrides are predicted to have T_C values above 200 K,[18,39–42] with some of them exhibiting superconductivity near room temperature and even higher.[21,22,43] Even more interestingly, these high-T_C hydrides (>200 K) contain diverse hydrogen configurations, such as isolated atomic hydrogen in covalent hydrides, two-dimensional (2D) H motifs, and various 3D H cages with covalent H–H bonding character.

It is worth noting that theoretical calculations play a crucial role in identifying conventional superconductors such as H_3S,[44,45] LaH_{10},[46–49] YH_9,[46,50] and PrH_9,[51] and provide effective guidance for

experimental synthesis.[52,53] Meanwhile, more and more advanced prediction methods are being developed, inevitably accelerating the development of hydride superconductors.[54–61] Theoretical calculations also have unique advantages in revealing the microscopic mechanism of superconductivity from both physical and chemical aspects, including chemical bonding, charge distribution, and electronic properties, as well as quantum effects.[62–65]

To gain insight into the features of high-T_C hydrides and provide inspiration for research on superconductors, in this review, the reported hydrides with T_C above 200 K are summarized with regard to their crystal structures, chemical bonds, electronic properties, and origin of superconductivity. The focus is mainly on covalent H_3S and several clathrate superhydrides (LaH_{10}, YH_9, and CaH_6) that have been predicted by theory and verified by experiment, although other theoretically predicted hydrides with clathrate H cages and 2D H motifs are also described. Finally, a comprehensive discussion and conclusions are presented, including a description of current problems and future challenges.

II. HIGH-PRESSURE COVALENT HYDRIDES

High-pressure covalent hydrides with T_C above 200 K are exemplified by *Im*-3*m* H_3S. The good agreement between experimental measurements[45,66] and theoretical calculations[44] provides a firm basis for the exploration of pressure-induced superconducting hydrides and for unveiling the mechanism of their superconductivity. In another important development, it has been demonstrated that the T_C value of H_3S can be significantly elevated via hole-doping.[43,67]

The high-T_C superconductivity of H_3S was observed in a high-pressure experiment aimed at verifying the predicted superconductivity of H_2S.[45] The T_C of 203 K and its pressure dependence are in good agreement with the theoretical prediction for *Im*-3*m* H_3S,[44] thus attracting great research interest. *Im*-3*m* H_3S contains body-centered cubic (bcc) S sites, and a nested [H_3S] sublattice in which each H atom bonds symmetrically with two S atoms forming a S-centered SH_6 octahedron [Fig. 1(a)], indicating the presence of atomic hydrogen.[68] Based on the weights of atomic orbitals, the large overlap of H *s* and S 3*p* orbitals below the Fermi level E_F indicates significant hybridization between them and the formation of a strong polar S–H covalent bond [Fig. 1(b)], which is consistent with the calculated electron localization function.[44] From its calculated electronic properties, H_3S is a good metal with a large density of states (DOS) peak near E_F and a band characterization of "flat band–steep band" [Fig. 1(b)]. Further, the Fermi surface for the single band contributing the main DOS near the E_F shows significant pockets [colored by the Fermi velocity in Fig. 1(c)].[64] These results demonstrate that *Im*-3*m* H_3S is a potential covalent metallicity-driven conventional superconductor. As expected, *Im*-3*m* H_3S is calculated to have strong electron–phonon coupling (EPC) with $\lambda = 2.19$, a large logarithmic average phonon frequency ω_{log} of 1334.6 K, and a high T_C value of 204 K at 200 GPa ($\mu^* = 0.1$). From the corresponding phonon density of states (PHDOS) and Eliashberg spectral function $\alpha^2F(\omega)$ [Fig. 1(d)], such a high T_C mainly originates from the large EPC contribution (82.6%) of a high-frequency hydrogen vibrational mode (>20 THz).[44]

Great effort has been made to further verify whether *Im*-3*m* H_3S is the source of high-T_C superconductivity in compressed H_2S. Extensive structural searches for S–H system with different stoichiometries indicate that H_2S becomes unstable and decomposes into H_3S and elemental β-Po sulfur above 43 GPa.[64,69] Specifically, pressure-induced metallic H_3S shows a phase transition from trigonal *R*3*m* to cubic *Im*-3*m* at 180 GPa. Moreover, the two phases of H_3S are estimated to have T_C values of 155–166 K for the *R*3*m* phase at 130 GPa and 191–204 K for the *Im*-3*m* structure at 200 GPa.[44] These theoretical results have been confirmed by synchrotron x-ray diffraction (XRD) combined with electrical resistance measurements [Figs. 1(e)–1(g)].[66] Therefore, the conclusion has been reached that cubic *Im*-3*m* H_3S is the primary contributor to the high T_C above 200 K in compressed H_2S owing to the metallicity driven by strong covalent bonds and the stabilization of atomic hydrogen by sulfur.[64,68] In addition, the quantum nature of the proton has a crucial effect on the stable pressure and symmetric hydrogen bonds in *Im*-3*m* H_3S.[63]

As an effective method to modulate superconductivity of materials,[70–73] atomic substitution is also performed to elevate the T_C of H_3S. The results demonstrate that partial substitution of S with P, C, and Si atoms significantly enhances the T_C to above 280 K.[43,67] In detail, the PDOS of *Im*-3*m* H_3S exhibits a conspicuous van Hove singularity below E_F [Fig. 1(b)], implying that hole doping probably moves the van Hove singularity to E_F, thus increasing the DOS at E_F and strengthening EPC. This can be realized by partial substitution of three kinds of atoms (e.g., P,[67] C,[43] and Si[43]) with fewer valence electrons than an S atom. Moreover, the DOS at E_F and the EPC constant first increase and then decrease with increasing doping content [Figs. 1(h), 1(i), and 1(k)]. Near room-temperature superconductivity is realized in $H_3S_{0.925}P_{0.075}$ ($T_C = 280$ K at 250 GPa),[67] $H_3S_{0.962}C_{0.038}$ ($T_C = 289$ K at 260 GPa), and $H_3S_{0.960}Si_{0.040}$ ($T_C = 283$ K at 230 GPa) [Figs. 1(j) and 1(l)].[67] Note that the pressure-dependent T_C values for P/C/Si-doped H_3S indicate that application of an appropriate pressure is also an important way to maximize the T_C of doped H_3S [Figs. 1(j) and 1(l)]. On the other hand, the high-T_C superconductivity of $H_3S_{0.962}C_{0.038}$ also provides a possible explanation for the recent experimental observation of room-temperature superconductivity in a highly compressed C–S–H system [Fig. 1(m)].[22]

III. CLATHRATE SUPERHYDRIDES

A. Experimentally verified LaH_{10}, YH_9, and CaH_6

Clathrate superhydrides comprise another important class of superconductors with T_C above 200 K. Typical representatives are *Fm*-3*m* LaH_{10},[47,48] $P6_3/mmc$ YH_9,[50] and *Im*-3*m* CaH_6,[74] which have been synthesized with direct guidance from theoretical predictions.[46,49,75] Their synthesis not only opens a potential route to achieving room-temperature superconductivity in clathrate superhydrides, but also indicates that other predicted high-T_C clathrate superhydrides might be successfully synthesized.

Fm-3*m* LaH_{10} is predicted to adopt a sodalite-like face-centered cubic (fcc) structure, in which each La atom is surrounded by a cage of 32 H atoms [Fig. 2(a)].[49] Each H-cage consists of 6 H-square and 12 H-hexagon rings, with two inequivalent H atoms, named H_1 and H_2. The H–H bond length is close to that of the predicted atomic metallic hydrogen near 500 GPa (1.0 Å),[9] indicating that H atoms are bonded to each other with covalent bonds.[65] As a result, all H vibrations can effectively participate in the EPC process, leading to strong EPC ($\lambda = 2.2$) and high T_C values of 257–274 K with $\mu^* = 0.1$–0.13 at 250 GPa.[49] This prediction has been verified by two experimental groups,[46,47] who have reported an La hydride $LaH_{10\pm x}$ ($x < 1$) with $T_C \approx 260$ K at about 190 GPa or 250 K at about 170 GPa [Fig. 2(e)].

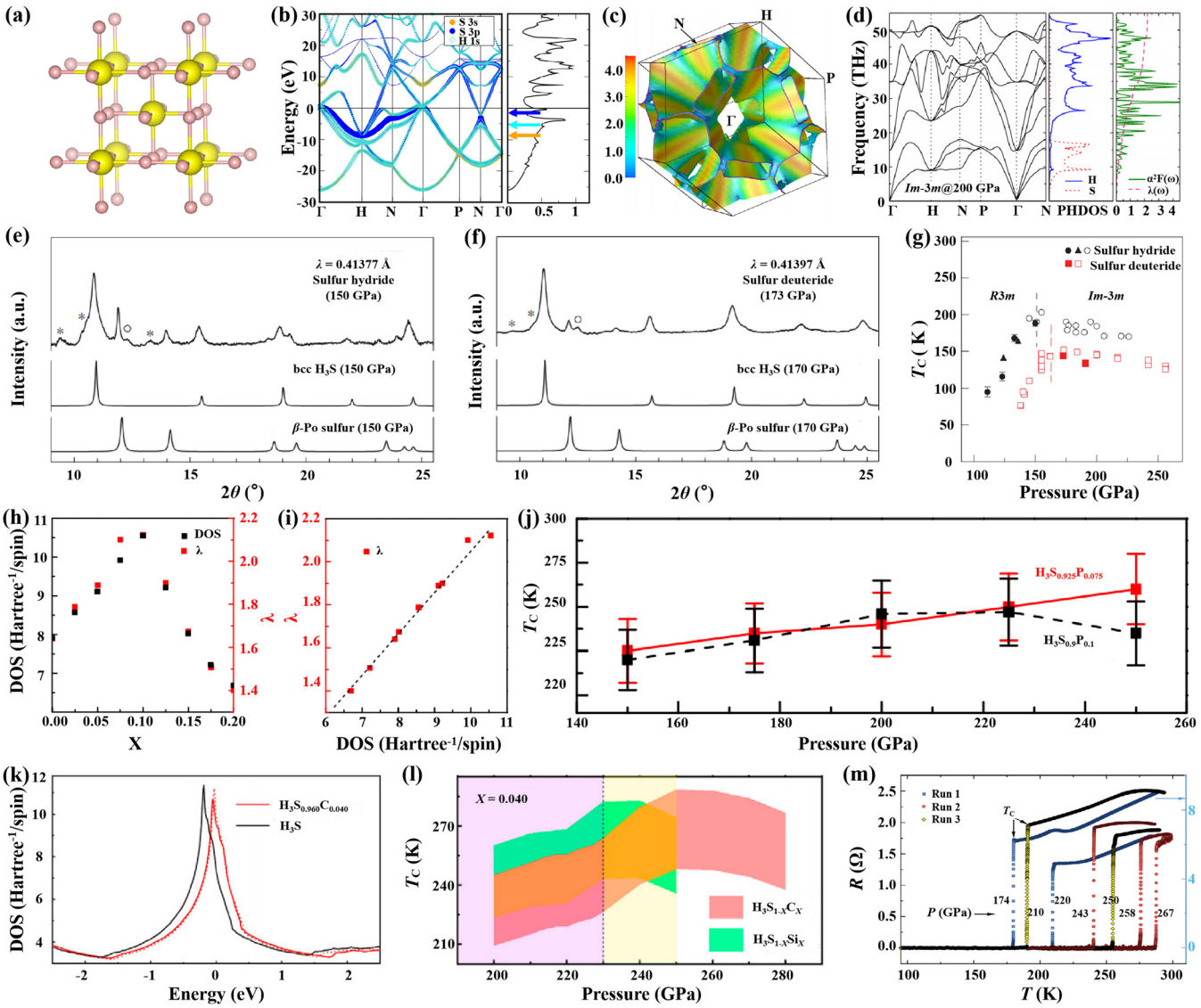

FIG. 1. (a) Crystal structure of *Im*-3*m* H_3S.[44] (b) Band structure of *Im*-3*m* H_3S.[64] (c) Main pocket of the Fermi surface of H_3S.[64] (d) Phonon dispersion curves and Eliashberg spectral function.[44] (e) and (f) Integrated XRD patterns obtained by subtraction of the background for sulfur hydride and sulfur deuteride, respectively.[66] (g) Pressure dependence of T_C of sulfur hydride (black points) and sulfur deuteride (red points).[66] (h) DOS and λ vs substitution concentration.[67] (i) Linear relationship between λ and DOS.[67] (j) T_C of $H_3S_{0.925}P_{0.075}$ (red solid line) and $H_3S_{0.9}P_{0.1}$ (black dashed line) vs pressure.[67] (k) DOS of H_3S at 220 GPa (black), $H_3S_{0.960}C_{0.040}$ at 220 GPa (solid red), and $H_3S_{0.960}C_{0.040}$ at 240 GPa (dashed red), with their Fermi energies set to be zero.[43] (l) T_C (shaded) vs pressure at $x = 0.040$.[43] (m) Temperature-dependent electrical resistance of the C–S–H system at high pressure.[22] (a) and (d) Reprinted with permission from Duan *et al.*, Sci. Rep. **4**, 6968 (2014). Copyright 2014 Nature Publishing Group. (b) and (c) Reprinted with permission from Bernstein *et al.*, Phys. Rev. B **91**, 060511 (2015). Copyright 2015 American Physical Society. (e)–(g) Reprinted with permission from Einaga *et al.*, Nat. Phys. **12**, 835 (2016). Copyright 2016 Nature Publishing Group. (h)–(j) Reprinted with permission from Ge *et al.*, Phys. Rev. B **93**, 224513 (2016). Copyright 2016 American Physical Society. (k) and (l) Reprinted with permission from Ge *et al.*, Mater. Today Phys. **15**, 100330 (2020). Copyright 2020 Elsevier. (m) Reprinted with permission from Snider *et al.*, Nature **586**, 373 (2020). Copyright 2020 Nature Publishing Group.

Furthermore, the bonding nature and superconducting mechanism of LaH_{10} have been extensively investigated. Intuitively, La atoms are thought to transfer charge to H atoms, suppressing the formation of H_2 molecules (extra charges occupy the antibonding orbitals).[49] However, based on the charge density of LaH_{10}, besides the H–H bonds, the La–H_1 bonds also exhibit covalent character from the connected charges between La and H_1 atoms [Fig. 2(b)]. The charge density difference also indicates charge accumulation in these regions.[65] In addition, on removing all H atoms in LaH_{10}, it was found that the metal framework of La atoms generates excess electrons in the interstitial regions, and

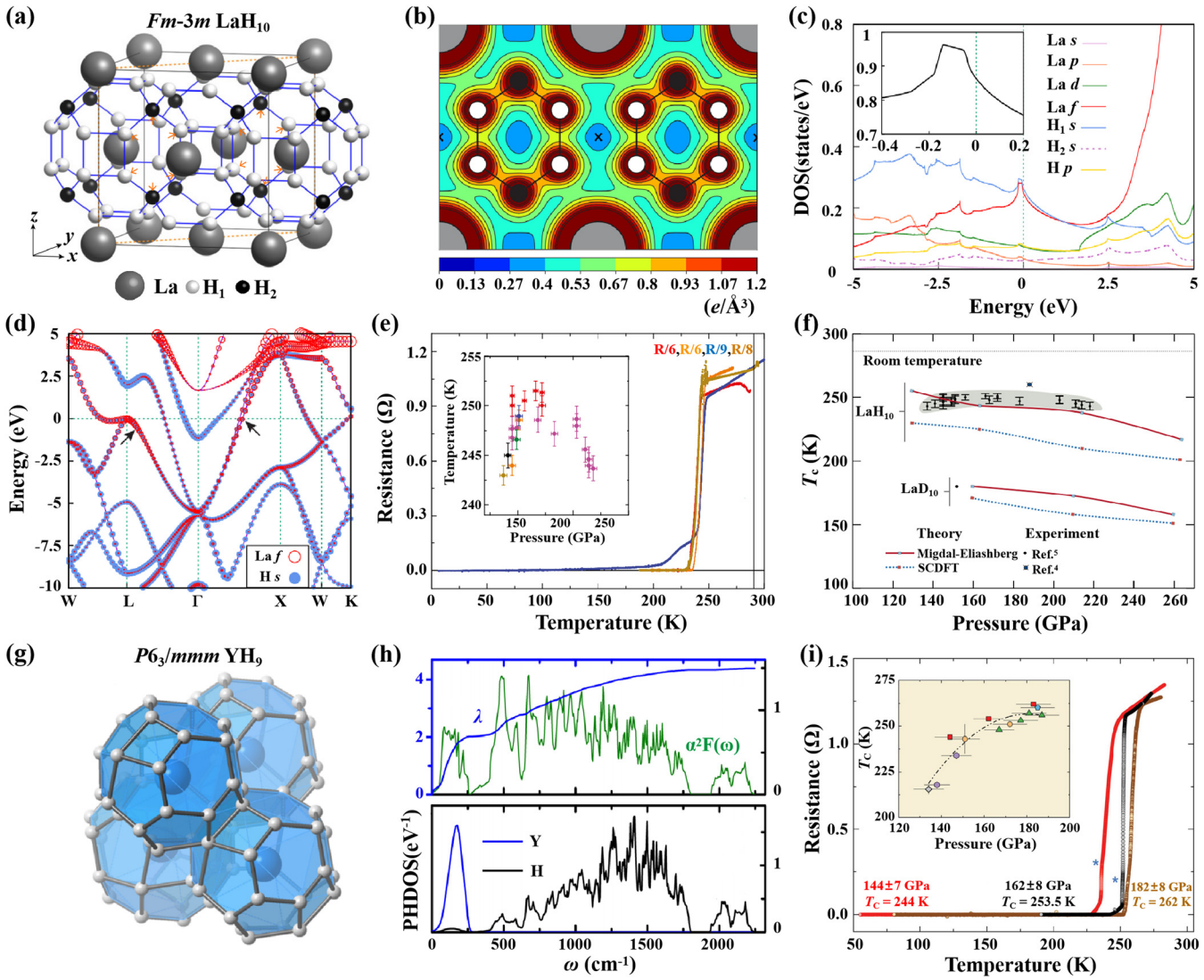

FIG. 2. (a) Structure of LaH_{10}.[65] (b) Total charge density ρ_{tot} of LaH_{10}.[65] (c) Partial DOS of LaH_{10}.[65] (d) Band structure of LaH_{10}.[65] (e) Observed superconductivity in LaH_{10}.[47] (f) Summary of experimental and theoretical T_C values in LaH_{10}.[62] (g) Structure of YH_9.[50] (h) Phonon spectra and Eliashberg spectral function for YH_9.[46] (i) Temperature-dependent electrical resistance of yttrium superhydride at high pressures.[50] (a)–(d) Reprinted with permission from Liu *et al.*, Phys. Rev. B **99**, 140501 (2019). Copyright 2019 American Physical Society. (e) Reprinted with permission from Drozdov *et al.*, Nature **569**, 528 (2019). Copyright 2019 Nature Publishing Group. (f) Reprinted with permission from Errea *et al.*, Nature **578**, 66 (2020). Copyright 2020 Nature Publishing Group. (g) and (i) Reprinted with permission from Snider *et al.*, Phys. Rev. Lett. **126**, 117003 (2021). Copyright 2021 American Physical Society. (h) Reprinted with permission from Peng *et al.*, Phys. Rev. Lett. **119**, 107001 (2017). Copyright 2017 American Physical Society.

transfers interstitial electrons to H cages, facilitating stabilization of LaH_{10}.[76,77] Therefore, the bonding nature between La atoms and H_{32} cages is characterized as mixed ionic–covalent bonding.[76]

On the other hand, there are two van Hove singularities with a separation of ~90 meV near E_F [Fig. 2(c)], originating from the hole-like and electron-like bands [Fig. 2(d)]. Specifically, the two bands arise from the splitting of the symmetry-protected topological states at the equivalent high-symmetry L points.[65] A high H-derived DOS at E_F and strong hybridization between La f and H_1 s orbitals are manifested in the DOS and band structure [Figs. 2(c) and 2(d)]. Moreover, the four Fermi surfaces corresponding to four bands crossing E_F exhibit strong coupling between the hybridized states (La and H_1 atoms as well as H_1 and H_2 atoms) and the phonon modes in the whole frequency range, giving rise to two nodeless, anisotropic superconducting gaps.[78] Consequently, the unusual bonding and electronic properties induce a highly optimized electron–phonon interaction that favors coupling to high-frequency hydrogen phonons,[79] and H-dominated high-T_C superconductivity in Fm-3m LaH_{10}.[80] In addition, the pressure dependence of EPC mainly accounts for the decrease in T_C with pressure,[80,81] supporting the

experimental measurements.[47] Notably, these characteristics are very similar to those of *Im*-3*m* H_3S, indicating some common features of high-T_C hydrides. Besides, as in H_3S, the inclusion of quantum effects in LaH_{10} brings the theoretically stable pressure and T_C values into better consistency with experimental measurements [Fig. 2(f)].[62]

Similar to *Fm*-3*m* LaH_{10}, several other pressure-induced superhydrides with H_{32} cages and the same symmetry have also been predicted to exhibit strong H-dominated EPC and high-T_C superconductivity above 200 K, such as YH_{10} with T_C = 303–326 K at 250–400 GPa,[46,49] Sc- or Y-substituted LaH_{10} with T_C enhanced compared with LaH_{10},[82] and TbH_{10} with T_C > 270 K at 250 GPa,[83] although these await experimental confirmation. However, not all LaH_{10}-type superhydrides have T_C above 200 K (e.g., T_C < 56 K for CeH_{10}[46,84] and T_C < 82 K for UH_{10}[85,86]), indicating that the particular metal atom has a vital effect on T_C even in the same hydrogen lattice framework.

Encouragingly, another predicted high-T_C clathrate superhydride, *P*6$_3$/*mmc* YH_9, has recently been synthesized.[46,50] In contrast to LaH_{10}, in *P*6$_3$/*mmc* YH_9, the Y atom is located in an H_{29} cage, consisting of six H-square, H-pentagon, and H-hexagon rings [Fig. 2(g)]. This densely packed arrangement leads to a much-reduced ΔPV term, stabilizing the structure. The large DOS contributed by Y *d* and H *s* orbitals and two van Hove singularities near E_F induce strong EPC (λ = 4.42) and a high T_C value of 276 K (μ^* = 0.1) at 150 GPa [Fig. 2(h)], which has been unambiguously verified in a recent experiment[50] [Fig. 2(i)]. Note that the Y atoms contribute a large EPC fraction of 45%. Interestingly, *P*6$_3$/*mmc* ScH_9 is predicted to have a lower T_C (<200 K at 120 GPa) than YH_9, although Sc has a lower atomic weight than Y. On the other hand, PrH_9[51] and ThH_9,[87] which are isostructural to YH_9, also have much lower T_C values of 8.9 K at 120 GPa and 145 K at 150 GPa, respectively.

Beside LaH_{10}-type and YH_9-type structures, there is also a class of experimentally verified high-T_C clathrate superhydrides with a sodalite-like bcc structure with *Im*-3*m* symmetry. In fact, CaH_6 with *Im*-3*m* symmetry is the first predicted clathrate superhydride with

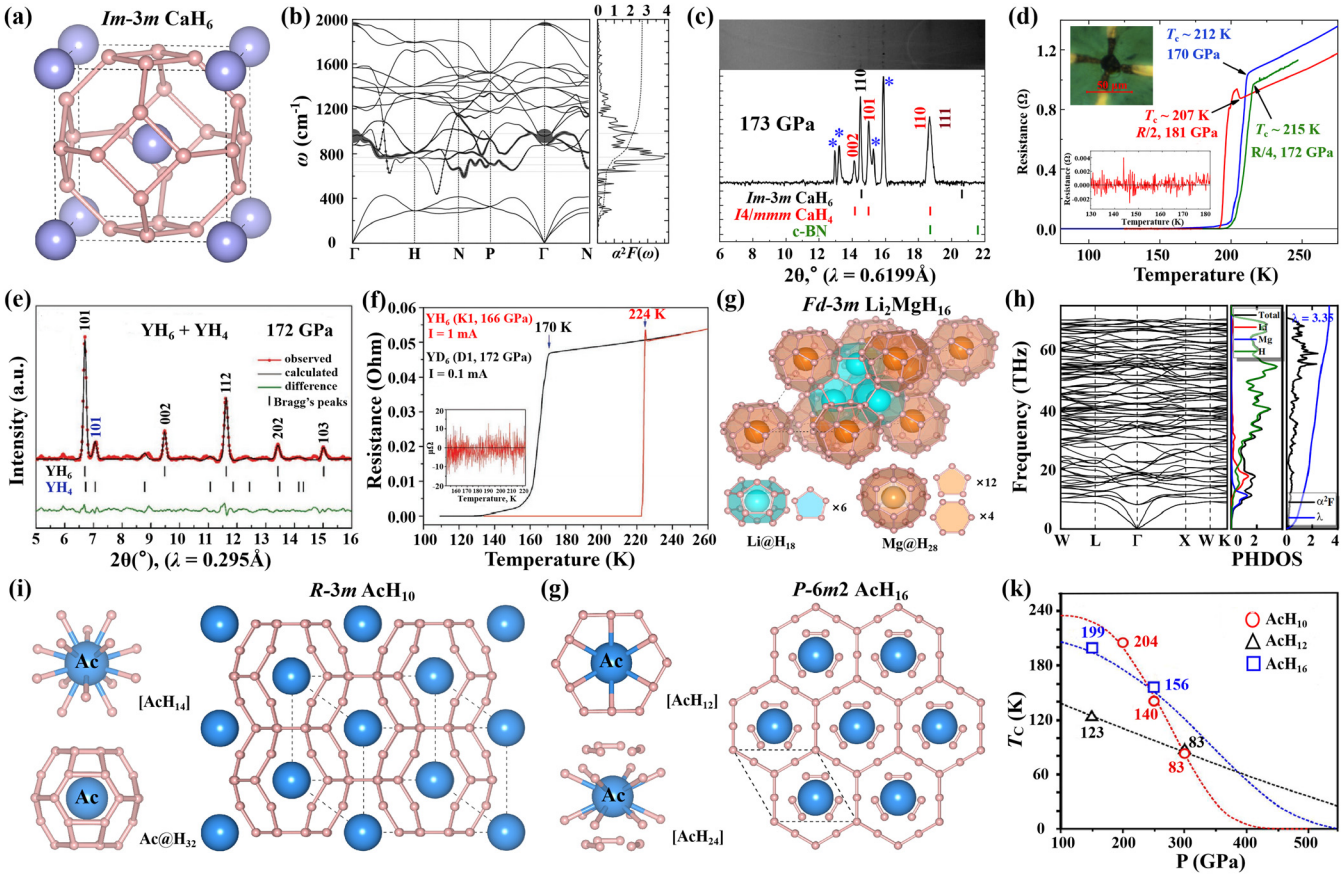

FIG. 3. (a) Structure of CaH_6.[75] (b) Phonon dispersion relation and Eliashberg spectral function.[75] (c) Synchrotron XRD pattern of superconducting calcium hydrides.[74] (d) Superconducting measurements in the calcium hydride CaH_x.[74] (e) XRD patterns and Le Bail refinements of *Im*-3*m* YH_6 and *I*4/*mmm* YH4.[91] (f) Temperature dependence of electrical resistance in YH_6 and YD_6.[91] (g) Structure of Li_2MgH_{16}.[21] (h) Phonon dispersion relations, projected phonon densities of states (PHDOS), and Eliashberg spectral function.[21] (i) Structure of AcH_{10}.[94] (j) Structure of AcH_{16}.[94] (k) T_C(P) functions.[94] (a) and (b) Reprinted with permission from Wang *et al.*, Proc. Natl. Acad. Sci. U. S. A. **109**, 6463 (2012). Copyright 2012 Proceedings of the National Academy of Sciences of the United States of America. (c) and (d) Reprinted with permission from Ma *et al.*, arXiv:2103.16282v2 (2021). (e) and (f) Reprinted with permission from Troyan *et al.*, Adv. Mater. **33**, 2006832 (2021). Copyright (2021) Wiley-VCH. (g) and (h) Reprinted with permission from Sun *et al.*, Phys. Rev. Lett. **123**, 097001 (2019). Copyright (2019) American Physical Society. (i)–(k) Reprinted with permission from Semenok *et al.*, J. Phys. Chem. Lett. **9**, 1920 (2018). Copyright (2018) American Chemical Society.

T_C > 200 K.[75] In this kind of structure, the metal atoms possess a bcc configuration, and are accommodated in H_{24} cages consisting of six H-square and eight H-hexagon rings [Fig. 3(a)]. A high phonon frequency and large DOS at E_F induce strong H-dominated EPC [Fig. 3(b)] and high T_C, with examples including CaH_6 with T_C of 220–235 K at 150 GPa,[75] MgH_6 with T_C of about 260 K above 300 GPa,[88] and YH_6 with T_C of 251–264 K at 120 GPa.[89] Again, *Im*-3*m* ScH_6 has a lower T_C (169 K at 350 GPa) than YH_6.[90] What is noteworthy is that CaH_6 and YH_6 have been successfully synthesized,[74,91] as demonstrated by the XRD and temperature-dependent electrical resistances [Figs. 3(c)–3(g)]. These remarkable achievements provide an effective route to develop more high-T_C superconductors through combining theoretical predictions with experimental syntheses. More interestingly, two phases (namely, *Pm*-3*m* and *Fd*-3*m*) of $CaYH_{12}$, with the same hydrogen cage as CaH_6, are predicted to have T_C values up to 230 and 258 K, respectively.[92,93]

B. Other theoretically predicted clathrate superhydrides

In addition to the three classes of clathrate superhydrides described above (i.e., LaH_{10}-type with H_{32} cage,[49] YH_9-type with H_{29} cage,[46] and CaH_6-type with H_{24} cage[75]), other varieties of clathrate superhydrides are also predicted to exhibit high-T_C superconductivity above 200 K. One outstanding example is the recently predicted *Fd*-3*m* Li_2MgH_{16}.[21] Based on the idea that electron doping is expected to lead to occupation of the antibonding orbital of H–H covalent bonds and the breakup of H_2 molecules, Li is introduced into binary MgH_{16} with large numbers of H_2 units, achieving atomic hydrogen cages [Fig. 3(g)]. Each Li atom is surrounded by one H_{18} cage, which is opened to connect to neighboring H_{18} cages. Each Mg atom is situated in one closed H_{28} cage. It has been proposed that a pyrochlore-type Li framework provides electrons to H-cages by forming electrides, not only stabilizing the clathrate H cages but also enhancing the H-dominated DOS at E_F.[77] As a result, Li_2MgH_{16} is predicted have strong EPC (λ = 3.35) and a superhigh T_C of 351 K at 300 GPa [Fig. 3(h)] and even as high as ~473 K at 250 GPa.

Despite being in the same group as La, the reaction of Ac with H_2 is predicted to result in two stable high-T_C compositions, namely, AcH_{10} and AcH_{16}.[94] *R*-3*m* AcH_{10} with H_{32} cages is in sharp contrast with *Fm*-3*m* LaH_{10} [Fig. 3(i)]. The shortest H–H distance in *R*-3*m* AcH_{10} is 1.07 Å at 150 GPa. For *P*-6*m*2 AcH_{16} with higher H content, each Ac atom is surrounded by 12 H atoms and 6 H_2 molecules with an H–H distance of 0.87 Å at 150 GPa [Fig. 3(j)]. Meanwhile, the H

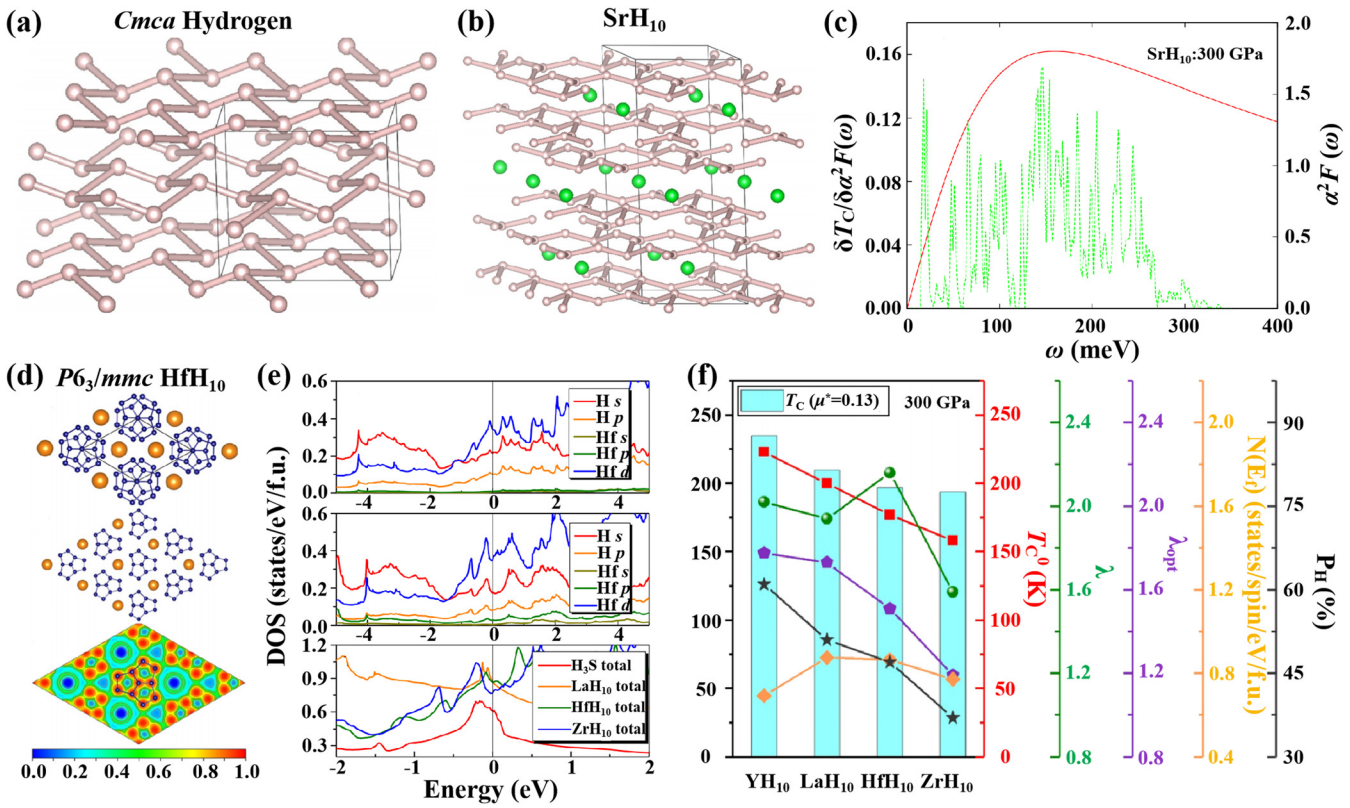

FIG. 4. (a) *Cmca* structure of molecular hydrogen at 300 GPa.[95] (b) Structure of SrH_{10}.[95] (c) $\delta T_C/\delta\alpha^2F(\omega)$ (red solid curve) and $\alpha^2F(\omega)$ (green dashed curve) as functions of frequency ω for SrH_{10} at 300 GPa.[95] (d) Structure of HfH_{10} and electron localization function on the (001) plane.[96] (e) Projected electronic DOS of HfH_{10} and ZrH_{10} and total electronic DOS of H_3S, LaH_{10}, HfH_{10}, and ZrH_{10}.[96] (f) Superconducting parameters for YH_{10}, LaH_{10}, HfH_{10}, and ZrH_{10}.[96] (a)–(c) Reprinted with permission from Tanaka *et al.*, Phys. Rev. B **96**, 100502 (2017). Copyright 2017 American Physical Society. (d)–(f) Reprinted with permission from Xie *et al.*, Phys. Rev. Lett. **125**, 217001 (2020). Copyright (2020) American Physical Society.

atoms form hexagonal H_{12} rings in the *ab* plane. In fact, in the bond length range of <1.3 Å, all H atoms form two kinds of cages: one is the empty H_{14} cage, and the other is the opened H_{36} cage surrounding the Ac atom. The two structures are estimated to exhibit strong EPC and high T_C values of 251 K at 200 GPa for AcH_{10} and 241 K at 150 GPa for AcH_{16} [Fig. 3(k)]. In addition, their T_C values decrease monotonically with pressure.[94]

IV. TWO-DIMENSIONAL HYDROGEN CONFIGURATION

Just as a cage structure is not the only structural motif that can support strong EPC, a 2D hydrogen configuration has also been predicted to lead to high-T_C superconductivity, such as in the *Cmca* metallic phase of solid hydrogen with $T_C = 242$ K at 450 GPa.[4] To date, two types of superhydrides with 2D hydrogen configuration have also been predicted to have high T_C values above 200 K, examples of which include SrH_{10}[95] and HfH_{10}.[96]

Similar to solid *Cmca* hydrogen [Fig. 4(a)], SrH_{10} also has puckered honeycomb H layers with H–H bond lengths between 0.998 and 1.011 Å, with Sr atoms being inserted into the interlayers [Fig. 4(b)].[95] The continuous phonon modes and Eliashberg spectral function in the whole frequency range [Fig. 4(c)] induce strong EPC ($\lambda = 3.08$) and a high T_C of 259 K at 300 GPa. On the other hand, it has recently been proposed that a planar pentagraphene-like hydrogen motif can be stabilized by Hf, Zr, Sc, or Lu atoms, forming novel 2D H_{10} units via H–H covalent bonds [Fig. 4(d)].[96] The metal atoms act as a precompressor and electron donor to the hydrogen sublattice. Metal *d* and H *s* and *p* orbitals are the main contributors to the DOS and generate distinct van Hove singularities, resulting in a large total DOS at E_F comparable to that of LaH_{10} [Fig. 4(e)]. Therefore, high-T_C superconductivity induced by strong EPC is obtained theoretically in HfH_{10} ($T_C = 234$ K at 250 GPa) and ZrH_{10} ($T_C = 220$ K at 250 GPa). Comparison with YH_{10} and LaH_{10} indicates that the high T_C values in these hydrides mainly originate from the interaction of electrons with optical phonons and the high DOS at E_F associated with H atoms [Fig. 4(f)]. By contrast, ScH_{10} and LuH_{10} are predicted to have lower T_C values of 158 K at 250 GPa and 152 K at 200 GPa, respectively.[96]

V. DISCUSSION AND CONCLUSION

On the whole, as predicted by Ashcroft,[12] a large number of hydrides have been found to exhibit high-T_C superconductivity above 200 K at lower pressures than are required for metallic hydrogen. Specifically, more and more theoretical predictions have been verified experimentally. In terms of the modes of arrangement of hydrogen atoms, these high-T_C hydrides (>200 K) contain different hydrogen configurations such as isolated hydrogen atoms in covalent hydrides, 2D planar and puckered hydrogen motifs, and 3D diverse hydrogen cages. In spite of the appearance of a variety of hydrogen configurations, one common feature of these hydrides is that all the hydrogen atoms form covalent bonds with hydrogen or other atoms, inducing significant H-contributed metallicity, strong EPC, and high-T_C superconductivity.

On the other hand, hydrogen is the simplest atom, and exhibits explicit bonding behavior at ambient pressure, but its bonding mechanism under high pressure is rather complex and even unconventional. For instance, how does pressure induce H atoms to form various cages via covalent bonding? These H configurations are completely different from those in the molecular phase at ambient pressure. How do different metal atoms affect H–H covalent bonds and superconductivity in the same hydrogen lattice framework? How do different metal atoms give rise to the formation of various hydrogen sublattices? These questions pose new challenges to high-pressure physics and chemistry.

The discovery of various binary hydrides with T_C above 200 K has provided a great stimulus to research into how these critical temperatures can be further raised via doping/substitution, as well as into ternary hydride superconductors. Exploration of ternary hydrides will surely lead to the prediction and synthesis of yet more high-T_C superconductors. The advances achieved with high-T_C hydrides not only indicate the great potential for achieving room-temperature superconductivity, but also provide a vast arena in which to study the formation mechanisms and physicochemical properties of novel hydrides under extreme conditions.

With the development of advanced synthetic methods and measurement techniques, as well as new theoretical methods, the day on which room-temperature superconductivity is finally achieved is getting closer. From the perspective of practical applications, the urgent task is to reduce the pressure required for stability of the hydrides while maintaining their high T_C values. On the other hand, the search for new structural types of superconductors provides an impetus for the development and enrichment of condensed matter theory.

ACKNOWLEDGMENTS

The authors acknowledge funding support from the Natural Science Foundation of China under Grant Nos. 21873017 and 21573037, the Postdoctoral Science Foundation of China under Grant No. 2013M541283, the Natural Science Foundation of Hebei Province (Grant No. B2021203030), and the Natural Science Foundation of Jilin Province (Grant No. 20190201231JC).

AUTHOR DECLARATIONS

Conflict of Interest

The authors have no conflicts to disclose.

Author Contributions

X.Z. and Y.Z. contributed equally to this paper.

REFERENCES

[1]H. Kamerlingh Onnes, "The superconductivity of mercury," Comm. Phys. Lab. Univ. Leiden **122**, 122 (1911).

[2]L. Gao, Z. J. Huang, R. L. Meng, J. G. Lin, F. Chen, L. Beauvais, Y. Y. Sun, Y. Y. Xue, and C. W. Chu, "Study of superconductivity in the Hg-Ba-Ca-Cu-O system," Physica C **213**, 261 (1993).

[3]L. Gao, Y. Y. Xue, F. Chen, Q. Xiong, R. L. Meng, D. Ramirez, C. W. Chu, J. H. Eggert, and H. K. Mao, "Superconductivity up to 164 K in $HgBa_2Ca_{m-1}Cu_mO_{2m+2+\delta}$ ($m = 1$, 2, and 3) under quasihydrostatic pressures," Phys. Rev. B **50**, 4260 (1994).

[4]P. Cudazzo, G. Profeta, A. Sanna, A. Floris, A. Continenza, S. Massidda, and E. K. U. Gross, "Ab initio description of high-temperature superconductivity in dense molecular hydrogen," Phys. Rev. Lett. **100**, 257001 (2008).

[5]L. Zhang, Y. Niu, Q. Li, T. Cui, Y. Wang, Y. Ma, Z. He, and G. Zou, "Ab initio prediction of superconductivity in molecular metallic hydrogen under high pressure," Solid State Commun. **141**, 610 (2007).

[6]H. Y. Geng, "Public debate on metallic hydrogen to boost high pressure research," Matter Radiat. Extremes **2**, 275 (2017).
[7]J. M. McMahon and D. M. Ceperley, "High-temperature superconductivity in atomic metallic hydrogen," Phys. Rev. B **84**, 144515 (2011).
[8]E. Gregoryanz, C. Ji, P. Dalladay-Simpson, B. Li, R. T. Howie, and H.-K. Mao, "Everything you always wanted to know about metallic hydrogen but were afraid to ask," Matter Radiat. Extremes **5**, 038101 (2020).
[9]N. W. Ashcroft, "Metallic hydrogen: A high-temperature superconductor?," Phys. Rev. Lett. **21**, 1748 (1968).
[10]P. Cudazzo, G. Profeta, A. Sanna, A. Floris, A. Continenza, S. Massidda, and E. K. U. Gross, "Electron-phonon interaction and superconductivity in metallic molecular hydrogen. II. Superconductivity under pressure," Phys. Rev. B **81**, 134506 (2010).
[11]J. M. McMahon and D. M. Ceperley, "Erratum: High-temperature superconductivity in atomic metallic hydrogen," Phys. Rev. B **85**, 219902 (2012).
[12]N. W. Ashcroft, "Hydrogen dominant metallic alloys: High temperature superconductors?," Phys. Rev. Lett. **92**, 187002 (2004).
[13]S. Ying, L. Han-Yu, and M. Yan-Ming, "Progress on hydrogen-rich superconductors under high pressure," Acta Phys. Sin. **70**, 017407 (2021).
[14]J. A. Flores-Livas, L. Boeri, A. Sanna, G. Profeta, R. Arita, and M. Eremets, "A perspective on conventional high-temperature superconductors at high pressure: Methods and materials," Phys. Rep. **856**, 1 (2020).
[15]D. V. Semenok, I. A. Kruglov, I. A. Savkin, A. G. Kvashnin, and A. R. Oganov, "On distribution of superconductivity in metal hydrides," Curr. Opin. Solid State Mater. Sci. **24**, 100808 (2020).
[16]H. Wang, X. Li, G. Gao, Y. Li, and Y. Ma, "Hydrogen-rich superconductors at high pressures," Wiley Interdiscip. Rev.: Comput. Mol. Sci. **8**, e1330 (2018).
[17]H. Y. Lv, M. Chen, Y. Feng, W. J. Li, G. H. Zhong, and C. L. Yang, "Superconductivity of light-metal hydrides," J. Chin. Chem. Soc. **66**, 1246 (2019).
[18]U. Pinsook, "In search for near-room-temperature superconducting critical temperature of metal superhydrides under high pressure: A review," J. Met., Mater. Miner. **30**, 31 (2020).
[19]J. Ma, J. Kuang, W. Cui, J. Chen, K. Gao, J. Hao, J. Shi, and Y. Li, "Metal-element-incorporation induced superconducting hydrogen clathrate structure at high pressure," Chin. Phys. Lett. **38**, 027401 (2021).
[20]D. Duan, Y. Liu, Y. Ma, Z. Shao, B. Liu, and T. Cui, "Structure and superconductivity of hydrides at high pressures," Natl. Sci. Rev. **4**, 121 (2016).
[21]Y. Sun, J. Lv, Y. Xie, H. Liu, and Y. Ma, "Route to a superconducting phase above room temperature in electron-doped hydride compounds under high pressure," Phys. Rev. Lett. **123**, 097001 (2019).
[22]E. Snider, N. Dasenbrock-Gammon, R. McBride, M. Debessai, H. Vindana, K. Vencatasamy, K. V. Lawler, A. Salamat, and R. P. Dias, "Room-temperature superconductivity in a carbonaceous sulfur hydride," Nature **586**, 373 (2020).
[23]T. Muramatsu, W. K. Wanene, M. Somayazulu, E. Vinitsky, D. Chandra, T. A. Strobel, V. V. Struzhkin, and R. J. Hemley, "Metallization and superconductivity in the hydrogen-rich ionic salt $BaReH_9$," J. Phys. Chem. C **119,** 18007 (2015).
[24]S. Zhang, L. Zhu, H. Liu, and G. Yang, "Structure and electronic properties of Fe_2SH_3 compound under high pressure," Inorg. Chem. **55**, 11434 (2016).
[25]C. Kokail, W. von der Linden, and L. Boeri, "Prediction of high-T_c conventional superconductivity in the ternary lithium borohydride system," Phys. Rev. Mater. **1**, 074803 (2017).
[26]Y. Ma, D. Duan, Z. Shao, H. Yu, H. Liu, F. Tian, X. Huang, D. Li, B. Liu, and T. Cui, "Divergent synthesis routes and superconductivity of ternary hydride $MgSiH_6$ at high pressure," Phys. Rev. B **96**, 144518 (2017).
[27]M. Rahm, R. Hoffmann, and N. W. Ashcroft, "Ternary gold hydrides: Routes to stable and potentially superconducting compounds," J. Am. Chem. Soc. **139**, 8740 (2017).
[28]D. Li, Y. Liu, F.-B. Tian, S.-L. Wei, Z. Liu, D.-F. Duan, B.-B. Liu, and T. Cui, "Pressure-induced superconducting ternary hydride H_3SXe: A theoretical investigation," Front. Phys. **13**, 137107 (2018).
[29]X. Du, S. Zhang, J. Lin, X. Zhang, A. Bergara, and G. Yang, "Phase diagrams and electronic properties of B-S and H-B-S systems under high pressure," Phys. Rev. B **100**, 134110 (2019).
[30]K. S. Grishakov, N. N. Degtyarenko, and E. A. Mazur, "Electron, phonon, and superconducting properties of yttrium and sulfur hydrides under high pressures," J. Exp. Theor. Phys. **128**, 105 (2019).
[31]X. Liang, S. Zhao, C. Shao, A. Bergara, H. Liu, L. Wang, R. Sun, Y. Zhang, Y. Gao, Z. Zhao, X.-F. Zhou, J. He, D. Yu, G. Gao, and Y. Tian, "First-principles study of crystal structures and superconductivity of ternary YSH_6 and $LaSH_6$ at high pressures," Phys. Rev. B **100**, 184502 (2019).
[32]D. Meng, M. Sakata, K. Shimizu, Y. Iijima, H. Saitoh, T. Sato, S. Takagi, and S.-i. Orimo, "Superconductivity of the hydrogen-rich metal hydride Li_5MoH_{11} under high pressure," Phys. Rev. B **99**, 024508 (2019).
[33]S. Di Cataldo, W. von der Linden, and L. Boeri, "Phase diagram and superconductivity of calcium borohyrides at extreme pressures," Phys. Rev. B **102**, 014516 (2020).
[34]X. Guo, R.-L. Wang, H.-L. Chen, W.-C. Lu, K. M. Ho, and C. Z. Wang, "Stability and superconductivity of $TiPH_n$ (n = 1–8) under high pressure," Phys. Lett. A **384**, 126189 (2020).
[35]X. Li, Y. Xie, Y. Sun, P. Huang, H. Liu, C. Chen, and Y. Ma, "Chemically tuning stability and superconductivity of P–H compounds," J. Phys. Chem. Lett. **11**, 935 (2020).
[36]Y. Sun, Y. Tian, B. Jiang, X. Li, H. Li, T. Iitaka, X. Zhong, and Y. Xie, "Computational discovery of a dynamically stable cubic SH_3-like high-temperature superconductor at 100 GPa via CH_4 intercalation," Phys. Rev. B **101**, 174102 (2020).
[37]Y. Yan, T. Bi, N. Geng, X. Wang, and E. Zurek, "A metastable $CaSH_3$ phase composed of HS honeycomb sheets that is superconducting under pressure," J. Phys. Chem. Lett. **11**, 9629 (2020).
[38]S. Y. Lee, J.-Y. Hwang, J. Park, C. N. Nandadasa, Y. Kim, J. Bang, K. Lee, K. H. Lee, Y. Zhang, Y. Ma, H. Hosono, Y. H. Lee, S.-G. Kim, and S. W. Kim, "Ferromagnetic quasi-atomic electrons in two-dimensional electride," Nat. Commun. **11**, 1526 (2020).
[39]M. I. Eremets and A. P. Drozdov, "High-temperature conventional superconductivity," Phys.-Usp. **59**, 1154 (2016).
[40]Y. Yao and J. S. Tse, "Superconducting hydrogen sulfide," Chem. - Eur. J. **24**, 1769 (2018).
[41]E. Zurek and T. Bi, "High-temperature superconductivity in alkaline and rare earth polyhydrides at high pressure: A theoretical perspective," J. Chem. Phys. **150**, 050901 (2019).
[42]L. Boeri and G. B. Bachelet, "Viewpoint: The road to room-temperature conventional superconductivity," J. Phys.: Condens. Matter **31**, 234002 (2019).
[43]Y. Ge, F. Zhang, R. P. Dias, R. J. Hemley, and Y. Yao, "Hole-doped room-temperature superconductivity in $H_3S_{1-x}Z_x$ (Z = C, Si)," Mater. Today Phys. **15**, 100330 (2020).
[44]D. Duan, Y. Liu, F. Tian, D. Li, X. Huang, Z. Zhao, H. Yu, B. Liu, W. Tian, and T. Cui, "Pressure-induced metallization of dense $(H_2S)_2H_2$ with high-T_c superconductivity," Sci. Rep. **4**, 6968 (2014).
[45]A. P. Drozdov, M. I. Eremets, I. A. Troyan, V. Ksenofontov, and S. I. Shylin, "Conventional superconductivity at 203 kelvin at high pressures in the sulfur hydride system," Nature **525**, 73 (2015).
[46]F. Peng, Y. Sun, C. J. Pickard, R. J. Needs, Q. Wu, and Y. Ma, "Hydrogen clathrate structures in rare earth hydrides at high pressures: Possible route to room-temperature superconductivity," Phys. Rev. Lett. **119**, 107001 (2017).
[47]A. P. Drozdov, P. P. Kong, V. S. Minkov, S. P. Besedin, M. A. Kuzovnikov, S. Mozaffari, L. Balicas, F. F. Balakirev, D. E. Graf, V. B. Prakapenka, E. Greenberg, D. A. Knyazev, M. Tkacz, and M. I. Eremets, "Superconductivity at 250 K in lanthanum hydride under high pressures," Nature **569**, 528 (2019).
[48]M. Somayazulu, M. Ahart, A. K. Mishra, Z. M. Geballe, M. Baldini, Y. Meng, V. V. Struzhkin, and R. J. Hemley, "Evidence for superconductivity above 260 K in lanthanum superhydride at megabar pressures," Phys. Rev. Lett. **122**, 027001 (2019).
[49]H. Liu, I. I. Naumov, R. Hoffmann, N. W. Ashcroft, and R. J. Hemley, "Potential high-T_c superconducting lanthanum and yttrium hydrides at high pressure," Proc. Natl. Acad. Sci. U. S. A. **114**, 6990 (2017).
[50]E. Snider, N. Dasenbrock-Gammon, R. McBride, X. Wang, N. Meyers, K. V. Lawler, E. Zurek, A. Salamat, and R. P. Dias, "Synthesis of yttrium superhydride superconductor with a transition temperature up to 262 K by catalytic hydrogenation at high pressures," Phys. Rev. Lett. **126**, 117003 (2021).

[51]D. Zhou, D. V. Semenok, D. Duan, H. Xie, W. Chen, X. Huang, X. Li, B. Liu, A. R. Oganov, and T. Cui, "Superconducting praseodymium superhydrides," Sci. Adv. **6**, eaax6849 (2020).
[52]J. Lv, Y. Sun, H. Liu, and Y. Ma, "Theory-orientated discovery of high-temperature superconductors in superhydrides stabilized under high pressure," Matter Radiat. Extremes **5**, 068101 (2020).
[53]V. Struzhkin, B. Li, C. Ji, X.-J. Chen, V. Prakapenka, E. Greenberg, I. Troyan, A. Gavriliuk, and H.-k. Mao, "Superconductivity in La and Y hydrides: Remaining questions to experiment and theory," Matter Radiat. Extremes **5**, 028201 (2020).
[54]C. W. Glass, A. R. Oganov, and N. Hansen, "USPEX—Evolutionary crystal structure prediction," Comput. Phys. Commun. **175**, 713 (2006).
[55]A. O. Lyakhov, A. R. Oganov, H. T. Stokes, and Q. Zhu, "New developments in evolutionary structure prediction algorithm USPEX," Comput. Phys. Commun. **184**, 1172 (2013).
[56]Y. Yao, J. S. Tse, and K. Tanaka, "Metastable high-pressure single-bonded phases of nitrogen predicted via genetic algorithm," Phys. Rev. B **77**, 052103 (2008).
[57]Y. Wang, J. Lv, L. Zhu, and Y. Ma, "Crystal structure prediction via particle-swarm optimization," Phys. Rev. B **82**, 094116 (2010).
[58]Y. Wang, J. Lv, L. Zhu, and Y. Ma, "CALYPSO: A method for crystal structure prediction," Comput. Phys. Commun. **183**, 2063 (2012).
[59]D. C. Lonie and E. Zurek, "XtalOpt: An open-source evolutionary algorithm for crystal structure prediction," Comput. Phys. Commun. **182**, 372 (2011).
[60]K. J. Michel and C. Wolverton, "Symmetry building Monte Carlo-based crystal structure prediction," Comput. Phys. Commun. **185**, 1389 (2014).
[61]K. Xia, H. Gao, C. Liu, J. Yuan, J. Sun, H.-T. Wang, and D. Xing, "A novel superhard tungsten nitride predicted by machine-learning accelerated crystal structure search," Sci. Bull. **63**, 817 (2018).
[62]I. Errea, F. Belli, L. Monacelli, A. Sanna, T. Koretsune, T. Tadano, R. Bianco, M. Calandra, R. Arita, F. Mauri, and J. A. Flores-Livas, "Quantum crystal structure in the 250-kelvin superconducting lanthanum hydride," Nature **578**, 66 (2020).
[63]I. Errea, M. Calandra, C. J. Pickard, J. R. Nelson, R. J. Needs, Y. Li, H. Liu, Y. Zhang, Y. Ma, and F. Mauri, "Quantum hydrogen-bond symmetrization in the superconducting hydrogen sulfide system," Nature **532**, 81 (2016).
[64]N. Bernstein, C. S. Hellberg, M. D. Johannes, I. I. Mazin, and M. J. Mehl, "What superconducts in sulfur hydrides under pressure and why," Phys. Rev. B **91**, 060511 (2015).
[65]L. Liu, C. Wang, S. Yi, K. W. Kim, J. Kim, and J.-H. Cho, "Microscopic mechanism of room-temperature superconductivity in compressed LaH_{10}," Phys. Rev. B **99**, 140501 (2019).
[66]M. Einaga, M. Sakata, T. Ishikawa, K. Shimizu, M. I. Eremets, A. P. Drozdov, I. A. Troyan, N. Hirao, and Y. Ohishi, "Crystal structure of the superconducting phase of sulfur hydride," Nat. Phys. **12**, 835 (2016).
[67]Y. Ge, F. Zhang, and Y. Yao, "First-principles demonstration of superconductivity at 280 K in hydrogen sulfide with low phosphorus substitution," Phys. Rev. B **93**, 224513 (2016).
[68]D. A. Papaconstantopoulos, B. M. Klein, M. J. Mehl, and W. E. Pickett, "Cubic H_3S around 200 GPa: An atomic hydrogen superconductor stabilized by sulfur," Phys. Rev. B **91**, 184511 (2015).
[69]D. Duan, X. Huang, F. Tian, D. Li, H. Yu, Y. Liu, Y. Ma, B. Liu, and T. Cui, "Pressure-induced decomposition of solid hydrogen sulfide," Phys. Rev. B **91**, 180502 (2015).
[70]E. A. Ekimov, V. A. Sidorov, E. D. Bauer, N. N. Mel'nik, N. J. Curro, J. D. Thompson, and S. M. Stishov, "Superconductivity in diamond," Nature **428**, 542 (2004).
[71]K.-W. Lee and W. E. Pickett, "Superconductivity in boron-doped diamond," Phys. Rev. Lett. **93**, 237003 (2004).
[72]K. Sasmal, B. Lv, B. Lorenz, A. M. Guloy, F. Chen, Y.-Y. Xue, and C.-W. Chu, "Superconducting Fe-based compounds $(A_{1-x}Sr_x)Fe_2As_2$ with A = K and Cs with transition temperatures up to 37 K," Phys. Rev. Lett. **101**, 107007 (2008).
[73]S. A. J. Kimber, A. Kreyssig, Y.-Z. Zhang, H. O. Jeschke, R. Valentí, F. Yokaichiya, E. Colombier, J. Yan, T. C. Hansen, T. Chatterji, R. J. McQueeney, P. C. Canfield, A. I. Goldman, and D. N. Argyriou, "Similarities between structural distortions under pressure and chemical doping in superconducting $BaFe_2As_2$," Nat. Mater. **8**, 471 (2009).
[74]L. Ma, K. Wang, Y. Xie, X. Yang, Y. Wang, M. Zhou, H. Liu, G. Liu, H. Wang, and Y. Ma, "Experimental observation of superconductivity at 215 K in calcium superhydride under high pressures," arXiv:2103.16282 (2021).
[75]H. Wang, J. S. Tse, K. Tanaka, T. Iitaka, and Y. Ma, "Superconductive sodalite-like clathrate calcium hydride at high pressures," Proc. Natl. Acad. Sci. U. S. A. **109**, 6463 (2012).
[76]S. Yi, C. Wang, H. Jeon, and J.-H. Cho, "Stability and bonding nature of clathrate H cages in a near-room-temperature superconductor LaH_{10}," Phys. Rev. Mater. **5**, 024801 (2021).
[77]C. Wang, S. Yi, S. Liu, and J.-H. Cho, "Underlying mechanism of charge transfer in Li-doped MgH_{16} at high pressure," Phys. Rev. B **102**, 184509 (2020).
[78]C. Wang, S. Yi, and J.-H. Cho, "Multiband nature of room-temperature superconductivity in LaH_{10} at high pressure," Phys. Rev. B **101**, 104506 (2020).
[79]S. F. Elatresh, T. Timusk, and E. J. Nicol, "Optical properties of superconducting pressurized LaH_{10}," Phys. Rev. B **102**, 024501 (2020).
[80]D. A. Papaconstantopoulos, M. J. Mehl, and P. H. Chang, "High-temperature superconductivity in LaH_{10}," Phys. Rev. B **101**, 060506 (2020).
[81]C. Wang, S. Yi, and J.-H. Cho, "Pressure dependence of the superconducting transition temperature of compressed LaH_{10}," Phys. Rev. B **100**, 060502 (2019).
[82]M. Kostrzewa, K. M. Szczęśniak, A. P. Durajski, and R. Szczęśniak, "From LaH_{10} to room–temperature superconductors," Sci. Rep. **10**, 1592 (2020).
[83]Y.-L. Hai, N. Lu, H.-L. Tian, M.-J. Jiang, W. Yang, W.-J. Li, X.-W. Yan, C. Zhang, X.-J. Chen, and G.-H. Zhong, "Cage structure and near room-temperature superconductivity in TbH_n (n = 1–12)," J. Phys. Chem. C **125**, 3640 (2021).
[84]P. Tsuppayakorn-aek, U. Pinsook, W. Luo, R. Ahuja, and T. Bovornratanaraks, "Superconductivity of superhydride CeH_{10} under high pressure," Mater. Res. Express **7**, 086001 (2020).
[85]D. Wang, H. Zhang, H.-L. Chen, J. Wu, Q.-J. Zang, and W.-C. Lu, "Theoretical study on UH_4, UH_8 and UH_{10} at high pressure," Phys. Lett. A **383**, 774 (2019).
[86]X.-h. Wang, F.-w. Zheng, Z.-w. Gu, F.-l. Tan, J.-h. Zhao, C.-l. Liu, C.-w. Sun, J. Liu, and P. Zhang, "Hydrogen clathrate structures in uranium hydrides at high pressures," ACS Omega **6**, 3946 (2021).
[87]D. V. Semenok, A. G. Kvashnin, A. G. Ivanova, V. Svitlyk, V. Y. Fominski, A. V. Sadakov, O. A. Sobolevskiy, V. M. Pudalov, I. A. Troyan, and A. R. Oganov, "Superconductivity at 161 K in thorium hydride ThH_{10}: Synthesis and properties," Mater. Today **33**, 36 (2020).
[88]X. Feng, J. Zhang, G. Gao, H. Liu, and H. Wang, "Compressed sodalite-like MgH_6 as a potential high-temperature superconductor," RSC Adv. **5**, 59292 (2015).
[89]Y. Li, J. Hao, H. Liu, J. S. Tse, Y. Wang, and Y. Ma, "Pressure-stabilized superconductive yttrium hydrides," Sci. Rep. **5**, 9948 (2015).
[90]X. Ye, N. Zarifi, E. Zurek, R. Hoffmann, and N. W. Ashcroft, "High hydrides of scandium under pressure: Potential superconductors," J. Phys. Chem. C **122**, 6298 (2018).
[91]I. A. Troyan, D. V. Semenok, A. G. Kvashnin, A. V. Sadakov, O. A. Sobolevskiy, V. M. Pudalov, A. G. Ivanova, V. B. Prakapenka, E. Greenberg, A. G. Gavriliuk, I. S. Lyubutin, V. V. Struzhkin, A. Bergara, I. Errea, R. Bianco, M. Calandra, F. Mauri, L. Monacelli, R. Akashi, and A. R. Oganov, "Anomalous high-temperature superconductivity in YH_6," Adv. Mater. **33**, 2006832 (2021).
[92]H. Xie, D. Duan, Z. Shao, H. Song, Y. Wang, X. Xiao, D. Li, F. Tian, B. Liu, and T. Cui, "High-temperature superconductivity in ternary clathrate $YCaH_{12}$ under high pressures," J. Phys.: Condens. Matter **31**, 245404 (2019).
[93]X. Liang, A. Bergara, L. Wang, B. Wen, Z. Zhao, X.-F. Zhou, J. He, G. Gao, and Y. Tian, "Potential high-T_c superconductivity in $CaYH_{12}$ under pressure," Phys. Rev. B **99**, 100505 (2019).
[94]D. V. Semenok, A. G. Kvashnin, I. A. Kruglov, and A. R. Oganov, "Actinium hydrides AcH_{10}, AcH_{12}, and AcH_{16} as high-temperature conventional superconductors," J. Phys. Chem. Lett. **9**, 1920 (2018).
[95]K. Tanaka, J. S. Tse, and H. Liu, "Electron-phonon coupling mechanisms for hydrogen-rich metals at high pressure," Phys. Rev. B **96**, 100502 (2017).
[96]H. Xie, Y. Yao, X. Feng, D. Duan, H. Song, Z. Zhang, S. Jiang, S. A. T. Redfern, V. Z. Kresin, C. J. Pickard, and T. Cui, "Hydrogen pentagraphenelike structure stabilized by hafnium: A high-temperature conventional superconductor," Phys. Rev. Lett. **125**, 217001 (2020).